

# Automatic Variable Magnetic Flux Technique in Consequent Pole Type PM-Motor Utilizing Space Harmonic

Masahiro Aoyama/ IEEE Member

Department of Electrical and Electronics Engineering  
Shizuoka University  
3-5-1 Johoku, Naka-ku, Hamamatsu, Shizuoka Japan  
aoyama.masahiro@shizuoka.ac.jp

Toshihiko Noguchi/ IEEE Senior Member

Department of Electrical and Electronics Engineering  
Shizuoka University  
3-5-1 Johoku, Naka-ku, Hamamatsu, Shizuoka Japan  
noguchi.toshihiko@shizuoka.ac.jp

**Abstract**—This paper proposes a consequent pole type pancake-axial-gap variable magnetic flux PM-motor. The unique point of the proposed motor is that variable magnetic flux can be realized by the armature magnetomotive force, rotation speed and/or current phase. The back yokeless stator is adopted to constitute a series magnetic circuit, and the variable magnetic flux is realized by passively changing the magnetization amount of the image pole (iron pole) of the consequent pole structure. The magnetic circuit topology that realizes the above will be explained, and the magnetic circuit design of the optimum variable magnetic flux method will be studied by FE-analysis. In addition, the basic drive performance will be clarified by FE-analysis. Furthermore, the prototype for principle verification will be revealed.

**Keywords**—variable magnetic flux; pancake-axial-gap; magnetic circuit; consequent pole; self-excitation

## I. INTRODUCTION

In recent years, as global environmental regulations have been strengthened, an electrification is being promoted at the political level of each country as a trend towards a zero emissions society in the automotive application. Technological development of the 48-V mild hybrid system (48-V mild HEV) has been actively conducted, especially in Europe. Although the 48-V system is inferior in fuel efficiency improvement effect to the high voltage full HEV system, on the other hand, for a compact car, it is a compact, lightweight and inexpensive HEV system, which is easy to obtain cost advantages and fuel economy improvement effect. On the other hand, for low voltage driving, an Integrated Stator Generator (ISG)-system (P0-HEV) that combines a variable field magnetic claw pole type motor and an inverter is mainstream. However, in the case of the claw pole type motor, because of the separately excited type using the slip-ring, it is necessary to increase the field current more than before as the output becomes higher. As a result, abrasion and durability of the brush becomes a problem. On the HEV system side, the P2-HEV or P3-HEV system that can perform EV drive via the clutch shown in Fig. 1 (a) is superior to the P0-HEV system in fuel consumption improvement effect and power performance improvement effect [1]. In order to realize the P2-HEV system by adopting

the permanent magnet synchronous motor (PMSM) with high efficiency and high torque density in the 48-V system, it is limited to high torque and low speed assist type or assist type up to the low torque medium speed range with the transmission built-in. To solve the drawback of above problems, by adopting the variable magnetic flux PM-motor that has been actively researched and developed in recent years, it is possible to realize an assist type up to high torque and medium speed range, and the freedom of arrangement on invehicle layout is also increased. As a study of recent typical variable magnetic flux PM technique, there are A) a memory motor method that makes the magnet magnetic force of the PMSM variable [2]-[5], B) a method that adjusts the rotor skew angle [6],[7], C) a method that adjusts the magnetization amount of the iron pole of the consequent pole structure [8]-[11], D) a method that utilizing variable leakage magnetic flux [12]-[15], and E) a method of automatically flux weakening [16]. In the case of C) of Refs. [9]-[11], a high torque can be realized by enlarging the torque generation surface, but a chopper circuit for field winding control is necessary. In the case of D) of Refs. [12]-[14], the variable magnetic function is realized by devising the magnetic circuit design of the rotor while applying the conventional vector control as it is, without requiring a variable magnetic force magnet or an extra additional device, however, since the leakage magnetic flux is utilized, there is a problem that the variable field range is narrow. In the case of E), although the expansion of the torque generation surface and the

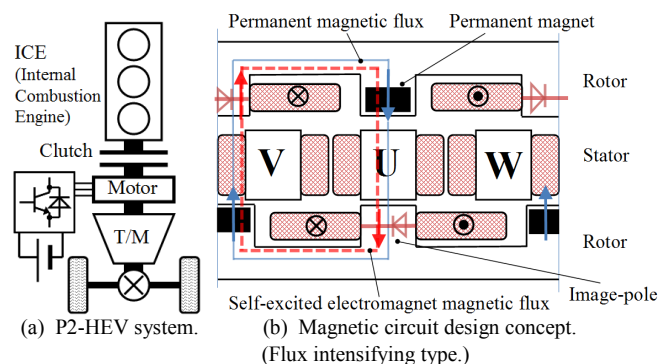


Fig. 1. HEV system of proposed motor application and magnetic circuit design concept. (with off-set rotor position.)

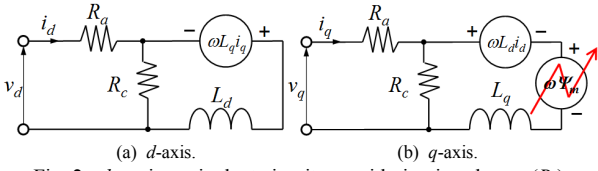


Fig. 2.  $dq$ -axis equivalent circuits considering iron losses ( $R_c$ ).

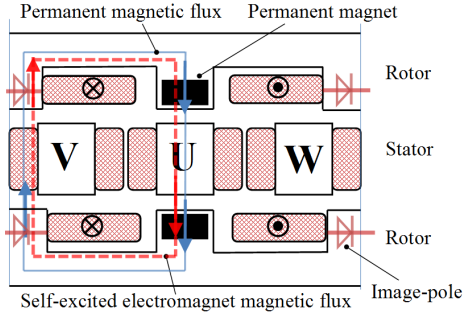


Fig. 3. Another magnetic pole placement type. (Flux intensifying type without off-set rotor position.)

passive variable magnetic field which requires no additional device are compatible, the structure is complicated.

In the contrast to the above technical problems, this paper proposes a pancake-axial-gap structure to realize expansion of the torque generation surface, and passively change the magnetic resistance of the image-pole (iron pole) of the consequent pole structure by the armature magnetomotive force and the rotation speed. Since passive variable magnetic flux technique does not require an additional device, e.g., DC/DC converter, cost merit is high. In this paper, the explanation of variable magnetic flux principle, study of magnetic circuit of proposed motor and drive performance prediction by FE-analysis are shown.

## II. VARIABLE MAGNETIC FLUX PRIPCIPLE

### A. Concept of Magnetic Circuit Design

Figure 1 (b) shows a schematic diagram of the magnetic circuit of the proposed motor. In order to realize high torque by enlarging the torque generation surface, a pancake-axial-gap structure is adopted. It adopts a consequent pole type rotor, and the image pole (iron pole) has a salient pole structure with winding a rotor coil, and it's rotor coil is a self-excited wound-field structure connected via a diode rectifier circuit. The induced electromotive force is generated when the second-order space harmonic which is unavoidably generated in the concentrated winding stator interlinks with the rotor winding, and the field current flows by the diode rectifier circuit with self-excitation [17]. The second-order space harmonic changes passively depending on the amplitude of the armature magnetomotive force. Since the induced electromotive force generated by the second-order space harmonic wave interlinking the rotor winding follows the Faraday's law, its electromotive force varies with the rotation speed. That is, the amount of magnetization of the image pole can be regarded as a variable field pole which passively changes with respect to the armature magnetomotive force and the rotation speed. As a result, in the  $dq$ -axis equivalent circuit shown in Fig. 2, the electromotive force due to the field magnetic flux of the  $q$ -axis

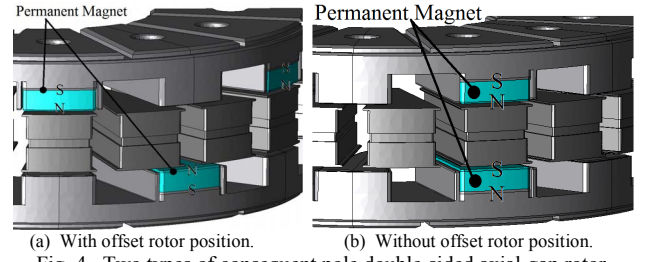


Fig. 4. Two types of consequent pole double-sided axial-gap rotor.

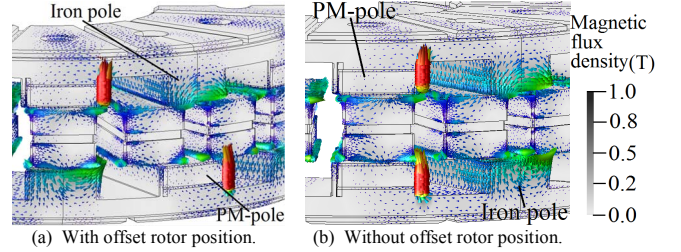


Fig. 5. Second-order space harmonic vectors.

equivalent circuit is variable, and variable field can be realized. On the other hand, by adopting the back yokeless segmented type concentrated winding stator structure, it is possible to efficiently link the second-order space harmonic occurring inevitably to both gap faces to the image pole [18]. According to Refs. [17] and [19], the second-order space harmonic that is inevitably generated in the concentrated winding stator is a magnetic field that rotates with 2-times harmonic of opposite phase with respect to the fundamental wave rotational coordinate, and when observed from the rotor (on the  $dq$ -axis) synchronously rotating with the fundamental rotating magnetic field, it becomes the third time harmonic. From Ref. [18] and above description, the magnetomotive force generated by concentrated winding stator structure can be explained by the following equations:

$$F_s(t, \theta) = \frac{3}{2} N I_a \left\{ R_{s1} \cos(\theta - \omega t + \delta) - \frac{1}{2} R_{s2} \cos(2\theta + \omega t - \delta) \right\} \quad (1)$$

where  $F_s$  is the magnetomotive force generated by concentrated winding stator structure,  $N$  is a turn number of armature coils,  $I_a$  is the amplitude of armature current,  $R_{s1}$  and  $R_{s2}$  is a amplitude of the fundamental content and a second-order space harmonic content of permeance distribution coefficient,  $\theta$  is a spatial position,  $\omega$  is an angular velocity,  $\delta$  is a armature current phase, respectively. As expressed in the above expression, the armature magnetomotive force of the concentrated winding stator is composed of fundamental rotating magnetic field and the other is a harmonic rotating magnetic field that rotates in the opposite phase direction at 2-times the speed with respect to fundamental rotating magnetic field. Then, applying a rotational coordinate transform by using the relationship in synchronous rotating state as  $\theta = \omega t$ , the second term in Eq. (1) is observed as a third time harmonic  $3\omega t$  on the  $dq$ -reference frame.

Slot combination is also an important factor. By setting the slot combination to 2-vs.-3 series, the rotor  $d$ -axis inductance varies with the three-order harmonic pulsation, so the magnetic coupling coefficient with the second-order space harmonic becomes strong [19]. Figure 4 shows the proposed model with

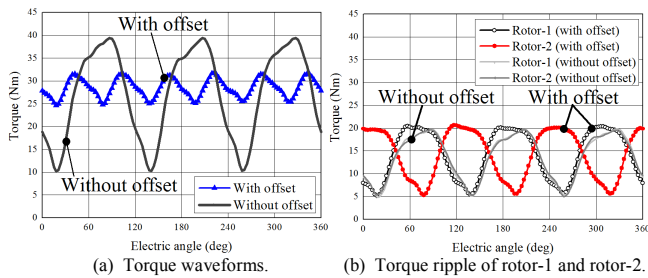


Fig. 6. Torque waveforms with rotor winding opened (FEA results).

the structure designed based on the magnetic circuit concept of Fig. 1 and Fig. 3. Figure 5 shows the second-order space harmonic vector distribution calculated by FE-analysis. As shown in Fig. 5, in either of the two magnetic pole arrangements, the second-order space harmonic is linked to the rotor salient pole (image pole), and when the coil is wound around the salient pole, the induced electromotive force can be obtained. On the other hand, as shown in Fig. 6 (a), the torque ripple greatly differs between the two magnetic pole arrangements. Generally, in the case of a consequent pole structure, there is a problem that the field pole having a field source (permanent magnet) and the image pole (iron pole) have a large difference in permeance and large torque ripple. However, in the case of the pancake-axial-gap structure, by offsetting the magnetic pole arrangement of the two rotors as shown in Fig. 4 (a), the phase relationship between the torque ripples of the two rotors becomes opposite in phase so that the torque ripple can be greatly reduced as shown in Fig. 6 (b). Therefore, Fig. 4 (a) is adopted for the magnetic pole arrangement of proposed motor.

### B. Self-Excited Wound-Field Pole

Next, as shown in Fig. 1, the polarity of the self-excited wound-field pole provided in the image pole can be set to the same polarity (flux intensifying) with respect to the magnet pole in the magnetic path of the series magnetic circuit configuration, or as shown in Fig. 7, the polarity is opposite (flux weakening). There are two possibilities. As described in the previous section, since the self-excited wound-field pole is a variable magnetic flux pole which passively changes with respect to the armature magnetomotive force and the rotation speed, in the former case, the magnetic flux is automatically increased. On the other hand, in the latter case, flux weakening is automatically performed as the rotation speed increases. Performance comparison of both type will be done in the next chapter. In this section, the principle verification machine used in the FE-analysis of the next chapter is shown. As shown in Fig. 8, the slot combination of 12 poles and 18 slots is adopted, and a high space factor is realized by inseting the performed rectangular wire wound coil which is shaped in flat angle alpha windings to eliminate the dead space occurring at the first turn of winding. A soft magnetic composite (SMC) is used for the three-dimensional magnetic path, and the segment type stator core is formed by splitting in the axial direction, and after being attached to a holding member made of SUS303 in Fig. 9, it is sealed with PPS resin. The rotor core is studied with a split core so that the weight density is about  $7.4 \sim 7.5 \text{ g/cm}^3$  with using a 600 ton press machine. Attach the rotor core to the protective member made of SUS303 in Fig. 9, then attach the

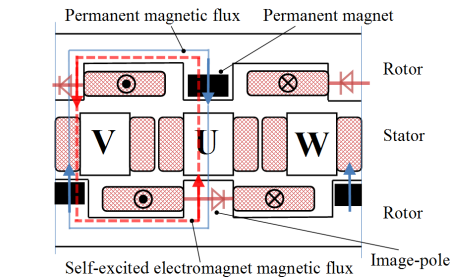


Fig. 7. Magnetic circuit design of flux weakening type.

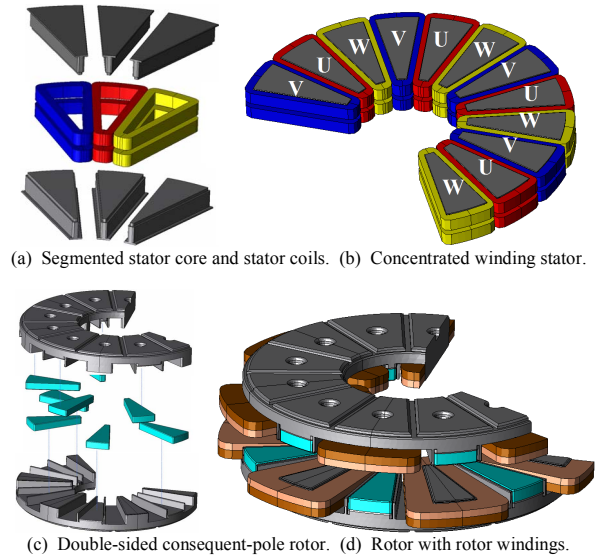


Fig. 8. Stator and rotor configurations.

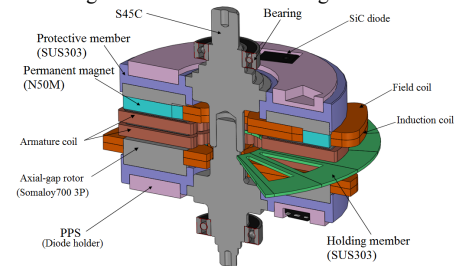


Fig. 9. Mechanical design of prototype machine.

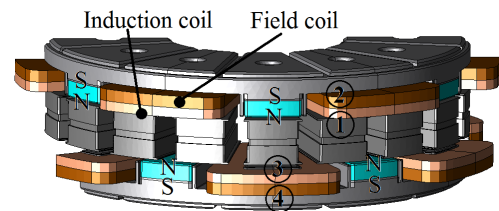


Fig. 10. Schematic of proposed motor with non-displayed armature windings.

permanent magnet (N50M manufactured by Shin-Etsu Chemical Co.) and the rotor winding, and next seal it with PPS resin. As shown in Fig. 9, the diode rectifier circuit is disposed on the rear face of the rotor by using a resin holder.

Next, the rotor rectifier circuit will be described with the flux intensifying type as an example. As can be confirmed in Fig. 5, since the second-order space harmonic of the self-excited energy source is distributed more in the gap face, as

shown in Fig. 10, an induction coil (I-coil) for obtaining induced electromotive force is arranged on the gap face, and the field coil (F-coil) for generating field magnetization is placed on the base of the rotor salient pole. As shown in Fig. 11 (a), since the induced electromotive force is generated in each I-coil by linking the second-order space harmonic, it is preferable that the rotor winding rectifier circuit is connected such that diodes are alternately conducting every half period and a positive voltage is output to the F-coil over the whole period. Thus, as shown in Fig. 11 (b) and (c), two I-coils are connected to the cathode common type diode, and the F-coil is arranged on the cathode side to constitute a rotor winding rectifier circuit. The I-coil and the F-coil are wound 90 turns each. Both the stator core and rotor core outer diameter are  $\phi 123$  mm, the air gap length is 0.8 mm, and the core axial length is 50 mm.

### III. PERFORMANCE PREDICTION BY ELECTROMAGNETIC FIELD ANALYSIS

#### A. Current Phase-vs.-Torque Characteristics

Firstly, the following analysis results were analyzed with a three-dimensional model using commercial electromagnetic field analysis software (JMAG-Designer ver. 16). In this study, in order to verify the performance difference due to the difference in the polarity of the variable field pole, various characteristics are considered in the constant torque region where the power supply voltage is sufficiently high. Figure 12 shows the current phase-vs.-torque characteristics at the rotation speed 2000 r/min and the armature magnetomotive force of 670 A<sub>rms</sub>T. As a reference, the result of placing the rotor winding rectifier circuit in the open state is also shown. Comparing the reference model with the other results from this figure, it can be confirmed that the torque is increased in the case of the same polarity with respect to the magnet poles, and the torque is decreased in the case of the opposite polarity. The magnetic resistance of the series magnetic circuit changes by changing the amount of magnetization of the image pole (iron pole) with the second-order space harmonic as the field energy source and the amount of magnetic flux interlinking the armature changes. Furthermore, it can be confirmed that the characteristics of the forward salient pole are obtained. Here, the  $+q$ -axis is defined as the current phase reference, and the  $-d$ -axis direction is defined as the phase advance side. Figure 13 shows the results of electromagnetic field analysis of the torque with respect to the armature magnetomotive force under the driving condition of the rotational speed of 2000 r/min and the current phase of 0 deg ( $i_d = 0$ ). In the case of  $i_d = 0$  control, only the magnet torque is obtained, and in the range where the magnetic saturation does not occur, the torque characteristic is linear with respect to the armature magnetomotive force. In the same figure, the reference model has a linear torque characteristic with respect to the armature magnetomotive force, whereas by setting to the variable magnetic flux type, it can be confirmed that the torque characteristic is nonlinear with respect to the armature magnetomotive force. From this, it is understood that the field amount of the self-excited wound-field pole can be passively adjusted by the armature magnetomotive force as described in Section 2.1. Figure 14 shows magnetic flux vector diagrams at a rotational speed of

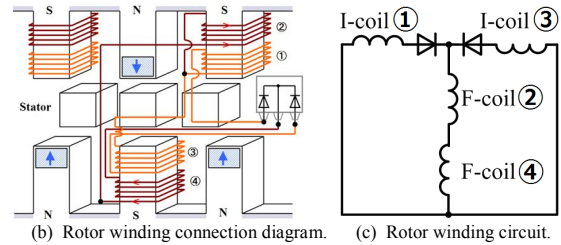
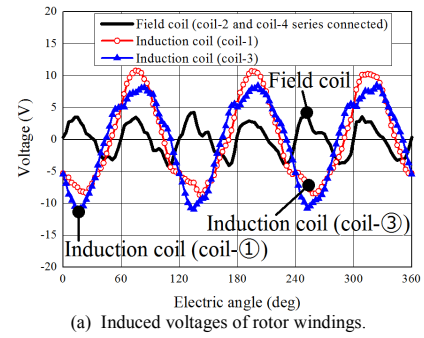


Fig. 11. Induced voltages and rotor winding circuit. (In case of flux intensifying type.)

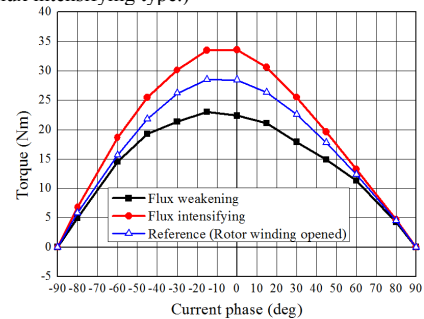


Fig. 12. Current phase-vs.-torque characteristics under 670 A<sub>rms</sub>T at 2000 r/min.

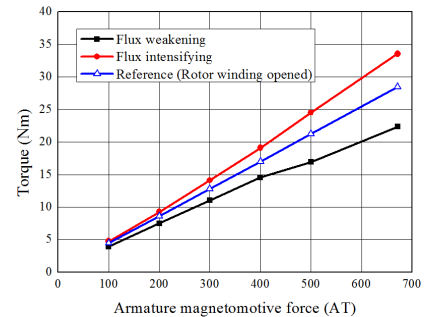


Fig. 13. Armature magnetomotive force-vs.-torque characteristics at 2000 r/min, and current phase 0 deg ( $i_d = 0$ ).

3000 r/min, the armature magnetomotive force of 670 A<sub>rms</sub>T and the current phase of 0 deg. From the figure, it can be confirmed that in the case of the flux intensifying type with respect to the reference model, the magnetic flux density of the image pole (iron pole) is high (magneto-resistance is low). On the other hand, in the case of the flux weakening type, it can be confirmed that the magnetic flux density of the image pole is lower than that of the reference model (high magneto-resistance). That is, it can be visually confirmed that the amount of magnetization of the self-excited wound-field pole wound on the image pole is passively changed by utilizing the space harmonic and variable field can be realized.

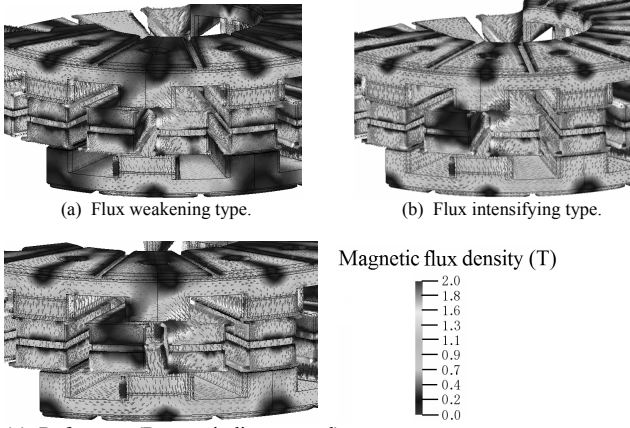


Fig. 14. Magnetic flux density and vectors under 670 A<sub>rms</sub>T, and current phase 0 deg ( $i_d = 0$ ) at 3000 r/min.

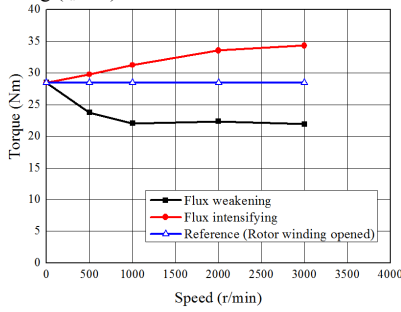


Fig. 15. Adjustable speed drive characteristics under 670 A<sub>rms</sub>T and current phase 0 deg ( $i_d = 0$ ).

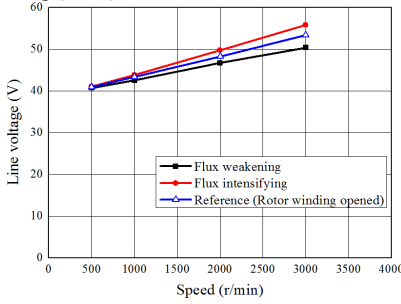


Fig. 16. Line voltages under 670 A<sub>rms</sub>T and current phase 0 deg ( $i_d = 0$ ).

### B. Adjustable Speed Drive Characteristics

Next, Fig. 15 shows the adjustable speed drive characteristics under the excitation condition of the armature magnetomotive force 670 A<sub>rms</sub>T and the current phase of 0 deg ( $i_d = 0$  control). In this case, in order to check the characteristics when the rotation speed changes under the constant armature magnetomotive force, the DC-bus voltage constraint is not considered. From this figure, in the case of the flux intensifying type, compared with the reference model, even under the constant condition of the armature magnetomotive force, the induced electromotive force at the rotor winding increases with the Faraday's law as the rotation speed increases, so that the magnetic flux strength of the iron pole increases. As a result, it can be confirmed that the torque is improved as the rotation speed increases. On the other hand, in the case of the flux weakening type, it can be seen that the torque decreases as the magnetic resistance of the iron pole increases as the rotation speed increases. It can be seen that in

both types, i.e., the flux intensifying type and the flux weakening type, as the rotation speed increases to some extent, the rate of change in the torque decreases. This is because the induced electromotive force generated by the interaction of the space harmonic with the rotor winding is opposed to the amount of superposition of the second-order space harmonic with respect to the fundamental wave. Figure 16 shows the variable magnetic flux effect to the line voltage. It can be seen from the figure that the change amount of the line voltage is smaller than the change amount of the torque. This is because the effect of the armature magnetic flux on the line voltage is larger than the magnet flux in the case of the consequent pole type. Here, the mathematical model of IPMSM is generally expressed by Eq. (2), and (3) on the  $dq$ -axis coordinate.

$$T = P_p \{ (L_d - L_q) i_d i_q + \psi_m i_q \} \quad (2)$$

$$\begin{bmatrix} v_d \\ v_q \end{bmatrix} = \begin{bmatrix} R + dL_d/dt & -\omega L_q \\ \omega L_d & R + dL_q/dt \end{bmatrix} \begin{bmatrix} i_d \\ i_q \end{bmatrix} + \begin{bmatrix} 0 \\ \omega \psi_m \end{bmatrix} \quad (3)$$

Here,  $P_p$  is the number of pole pair,  $d/dt$  is the differential operator,  $R$  is the armature winding resistance,  $L_d$ ,  $L_q$ ,  $i_d$ ,  $i_q$  are the  $dq$ -axis inductance,  $dq$ -axis armature current,  $\omega$  is the electrical angular velocity, and  $\psi_m$  is the magnetic flux of the magnet, respectively. In the case of the forward salient pole type ( $L_d > L_q$ ) like the proposed motor,  $v_d > v_q$ , and the  $q$ -axis becomes the  $dq$ -axis voltage ellipse with the long axis radius. In this case, the line voltage cannot be kept within the voltage ellipse by merely advancing the current phase angle by keeping the armature current vector norm constant in the rotation speed region above the nominal speed. It is necessary to drive by lowering the armature current vector norm. This will be described with reference to the  $dq$ -axis vector diagram. Figure 17 (a) and (b) show the  $dq$ -axis vector diagram of the flux weakening type and flux intensifying type. Here,  $\psi_{e-coil}$  is the electromagnet magnetic flux generated by at the self-excited wound-field pole with space harmonic as a field energy source. The vector shown in gray arrow in the figure is the case of the reference model. In the flux weakening type, the electromagnet flux vector in the opposite direction to the magnet flux vector is formed by the image pole (iron pole), and the magnetic resistance is increased. As a result, as shown in Fig. 17 (a), the  $dq$ -axis vector changes and the voltage  $V_s$  can be reduced. In the case of the flux intensifying type, the electromagnet flux vector in the same direction as the magnet flux vector is formed in the image pole (iron pole), and the magnetoresistance becomes small. As a result, the  $dq$ -axis vector changes as shown in Fig. 17 (b), and the voltage  $V_s$  increases. When it is desired to suppress the voltage with the flux intensifying type, since  $\psi_{e-coil}$  changes passively to the armature magnetomotive force, the flux intensifying field amount can be adjusted by lowering the armature current vector norm as shown in Fig. 17 (c). As described above, in the case of the forward salient pole type, since  $v_q > v_d$  and the  $q$ -axis is the  $dq$ -axis voltage ellipse with the long diameter radius, it is necessary to drive with lowering the armature current vector norm at or above the nominal rotation speed. This property means good compatibility with the variable magnetic flux adjustment of the flux intensifying type. In other words, in the region above the nominal rotation speed, adjusting the armature current vector

norm and finely adjusting the amount of field makes it possible to realize high torque and expand adjustable speed drive characteristics. Therefore, in the case of the variable magnetic flux motor proposed in this paper, it is good to design the image pole (iron pole) part with the flux intensifying type and adjust the operating point of the line voltage with the armature current vector norm.

#### IV. CONCLUSION

In this paper, it has been proposed that the motor which adopts a pancake-axial-gap structure to realize expansion of the torque generation surface and can passively change the magnetic resistance on the image pole (iron pole) of consequent pole structure by the armature magnetomotive force and the rotation speed. The explanation of the brushless variable magnetic flux principle on the image pole (iron pole) and the magnetic circuit design was explained, and the basic drive characteristics were clarified by electromagnetic field analysis. In addition, the performance consideration was made from the viewpoint of electromagnetic field analysis and vector diagram for the case where the variable field of the image pole is intensified and the case of flux weakening. As a result, in the case of the variable magnetic flux motor proposed in this paper, it is highly possible to improve the efficiency by improving the torque and reducing the armature copper loss by designing the image pole to be flux intensifying type and adjusting the line voltage by adjusting the armature current vector norm. In the future, the actual machine will be prototyped and actual drive characteristics, efficiency map, each losses, and variable magnetic flux ability will be demonstrated.

#### REFERENCES

[1] U. Keller, T. Godecke, M. Weiss, C. Enderle and G. Henning, "Diesel Hybrid - The Next Generation of Hybrid Powertrains by Mercedes-Benz -," 33rd International Vienna Motor Symposium 2012.

[2] V. Ostovic, "Memory Motors," IEEE Industry Applications Magazine, vol. 9, pp. 52-61, 2003.

[3] V. Ostovic, "Memory Motors - a New Class of Controllable Flux PM Machines for a True Wide Speed Operation," Proc. of IEEE Industry Applications Society Conference, vol. 4, pp. 2577-2584, 2001.

[4] K. Sakai, K. Yuki, Y. Hashiba, N. Takahashi and K. Yasui, "Principle of the Variable Magnetic-Force Memory Motor," IEEE Electrical Machines and Systems (ICEMS) 2009 International Conference on.

[5] T. Kato, N. Limsuwan, C. Y. Yu, K. Akatsu and R. D. Lorenz, "Rare Earth Reduction Using a Novel Variable Magnetomotive Force, Flux Intensified IPM Machine," IEEE Trans. on IA., vol. 5, no. 3, pp. 1748-1756, May/ June, 2016.

[6] T. Nonaka, S. Oga and M. Ohto, "Consideration about the Drive of Variable Magnetic Flux Motor," IEEJ Trans. on IA., vol. 135, no. 5, pp. 451-456, 2015. (in Japanese)

[7] K. Hiramoto, M. Namba, H. Nakai, K. Moriya, Y. Ito, T. Miura and K. Yamada, "Control Device of Rotary Electrical Machines and Its Motor Drive Control System," Patent release (A) 2015-177640, published in 2014. (in Japanese)

[8] T. Mizuno, K. Nagayama, T. Ashikaga and T. Kobayashi, "Basic Principles and Characteristics of Hybrid Excitation Synchronous Machine," Electrical Engineering in Japan, vol. 117, no. 5, pp. 110-123, 1996.

[9] J. A. Tapia, F. Leonardi and T. A. Lipo, "Consequent-Pole Permanent-Magnet Machine with Extended Field-Weakening Capability," IEEE Trans. on IA., vol. 39, no. 6, pp. 1704-1709, 2003.

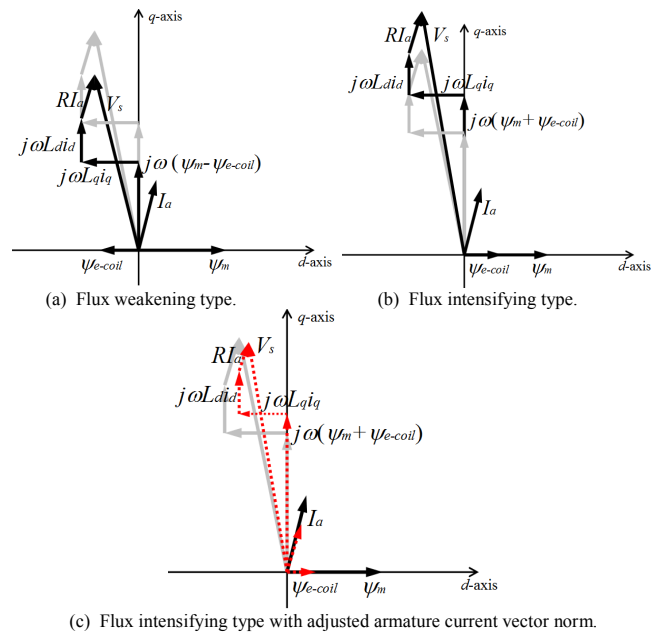


Fig. 17. Vector diagrams.

[10] T. Ogawa, T. Takahashi, M. Takemoto, H. Arita, A. Daikoku and S. Ogasawara, "The Consequent-Pole Type Ferrite Magnet Axial Gap Motor with Field Winding for Traction Motor Using in EV," SAEJ Proc. of 3rd International Electric Vehicle Technology & Automotive Power Electronics Japan Conference (EVTec & APE Japan 2016), no. 20169094.

[11] M. Namba, K. Hiramoto and H. Nakai, "Novel Variable-Field Machine with a Three-Dimensional Magnetic Circuit," IEEE Trans. on IA., vol. 53, no. 4, pp. 3404-3410, 2017.

[12] H. Hijikata, K. Akatsu and T. Kato, "Experimental Studies of Variable Leakage Flux Type IPMSM," IEEJ Trans. on IA., vol. 137, no. 9, pp. 737-743, 2017. (in Japanese)

[13] A. Athavale, T. Fukushige, T. Kato, C. Y. Yu and R. D. Lorenz, "Variable Leakage Flux (VLF) IPMSMs for Reduced Losses over a Driving Cycle while Maintaining the Feasibility of High Frequency Injection-Based Rotor Position Self-Sensing," IEEE Energy Conversion Congress and Exposition (ECCE), 2014.

[14] M. Minowa, H. Hijikata, K. Akatsu and T. Kato, "Variable Leakage Flux Interior Permanent Magnet Synchronous Machine for Improving Efficiency on Duty Cycle," IEEE International Power Electronics Conference (IPEC-Hiroshima 2014 - ECCE ASIA), 2014.

[15] I. Urquhart, D. Tanaka, R. Owen, Z. Q. Zhu, J. B. Wang and D. A. Stone, "Mechanically Actuated Variable Flux IPMSM for EV and HEV Applications," Proc. of EVS 27 International Battery, Hybrid and Fuel Cell Vehicle Symposium 2013, pp. 0684-0695, 2013.

[16] M. Aoyama, K. Nakajima and T. Noguchi, "Proposal and Preliminary Experimental Verification of Electrically Reversal Magnetic Pole Type Variable Magnetic Flux PM Motor," IEEJ Trans. on IA., vol. 137, no. 9, pp. 725-736, 2017. (in Japanese)

[17] M. Aoyama and T. Noguchi, "Experimental Verification of Radial-Air-Gap-Type Permanent-Magnet-Free Synchronous Motor Utilizing Space Harmonics with Auxiliary Poles," IEEJ Trans. on IA., vol. 135, no. 8, pp. 869-881, 2015. (in Japanese)

[18] M. Aoyama and T. Noguchi, "Proposal of Pancake Axial-Air-Gap-Type Self-Excited Wound-Field Synchronous Motor Utilizing Double-Sided Space Harmonics," IEEJ Trans. on IA., vol. 135, no. 5, pp. 582-583, 2015. (in Japanese)

[19] M. Aoyama and T. Noguchi, "Permanent-Magnet-Free-Synchronous Motor with Self-Excited Wound-Field Technique Utilizing Space Harmonics," Applied Power Electronics Conference and Exposition (APEC), 2017 IEEE, pp. 3187-3194, 2017.